Proceedings of IMECE2006
2006 ASME International Mechanical Engineering Congress and Exposition
November 5-10, 2006, Chicago, Illinois, USA

IMECE2006-15122

MODELING AND PARAMETRIC STUDY OF A CERAMIC HIGH TEMPERATURE HEAT EXCHANGER AND CHEMICAL DECOMPOSER

Valery Ponyavin[1,2], Yitung Chen[1,2], Taha Mohamed[1,2], Mohamed Trabia[2], Merrill Wilson[3], Anthony E. Hechanova[4]

[1]Nevada Center for Advanced Computational Methods, University of Nevada, Las Vegas
[2]Department of Mechanical Engineering, University of Nevada, Las Vegas
[3]Ceramatec, Inc., Salt Lake City
[4]Harry Reid Center for Environmental Studies, University of Nevada, Las Vegas
E-mail: ponyavin@nscee.edu

ABSTRACT

It is proposed to use ceramic high temperature heat exchanger as a sulfuric acid decomposer for hydrogen production within the sulfur iodine thermo-chemical cycle. The decomposer is manufactured using fused ceramic layers that allow creation of channels with dimensions below one millimeter. A three-dimensional computational model is developed to investigate the fluid flow, heat transfer, stresses and chemical reactions in the decomposer. Fluid, thermal and chemical reaction analyses are performed using FLUENT software. Temperature distribution in the solid is imported to ANSYS software and used together with pressure as the load for stress analysis. Results of this research can be used as a basis for investigation optimal design of the decomposer that can provide maximum chemical decomposition performance while maintaining stresses within design limits.

Keywords: *heat transfer, heat exchanger, stress analysis, ceramic material, silicon carbide*

NOMENCLATURE

A_r	pre-exponential factor
C_p	specific heat at constant pressure, $J \cdot kg^{-1} \cdot K^{-1}$
$D_{i,m}$	diffusion coefficient for species *i* in the mixture, $m^2 \cdot sec^{-1}$
M	molecular weight, $g \cdot mol^{-1}$
R	universal gas constant, $j \cdot mol^{-1} \cdot K^{-1}$
P_i	net rate of production of species *i* by chemical reaction, $kg \cdot m^{-3} \cdot sec^{-1}$
PM	overall factor of safety performance measure
S_i	rate of reaction of species i by addition from dispersed phase, $kg \cdot m^{-3} \cdot sec^{-1}$
T	static temperature, K
X_i	mass concentration of species i
fse_i	average factor of safety for each element *i*.
fsn_j	factor of safety for each of the eight nodes associated with element *i*.
$\dot{m}$	mass flow rate, $kg \cdot s^{-1}$
p	static pressure, Pa
s_{uc}	compressive strength, MPa
s_{ut}	tensile strength, MPa
t	time, s
u	velocity vector, $m \cdot s^{-1}$
v_i	volume of element *i*.
w_j	length coordinate i (x, y, z), m
ϕ	mole fraction
μ	dynamic viscosity, $kg \cdot m^{-1} \cdot s^{-1}$
ρ	density, $kg \cdot m^{-3}$

INTRODUCTION

Hydrogen can be an attractive energy carrier if it can be produced cleanly and in a cost-effective manner. Nuclear energy can be used as a source of energy for high temperature processes (up to 1000°C) for production of hydrogen. The Sulfur Iodine Cycle [1] is a baseline candidate thermo-chemical process. It consists of the following three chemical reactions which yield the dissociation of water:

$I_2+SO_2+2H_2O \rightarrow 2HI+H_2SO_4$ (120°C min.) (1)
$H_2SO_4 \rightarrow H_2O+SO_2+½O_2$ (850°C min.) (2)
$2HI \rightarrow H_2+I_2$ (450°C min.) (3)

The whole process takes in water and high-temperature heat, and releases hydrogen and oxygen (Figure 1). All reactions are in fluid interactions. All reagents are to be recycled; there are no effluents. Each of the chemical reactions in this process was demonstrated in the laboratory [2]. Japan Atomic Energy Research Institute developed a demonstration of the sulfur–iodine cycle [3],[4]. Decomposition of sulfuric acid and hydrogen iodide involve aggressive chemical environments. Hence, the material candidates for the sulfur–

iodine cycle hydrogen plant should be chosen carefully to accommodate corrosion problems as well.

One of the important and critical parts of the plant is the high temperature heat exchanger for SI (Sulfuric Acid) Processes - Preheater & Decomposer. The processes in the part of the plant are shown schematically in Figure 2, [5]. The SI decomposer is used as part of the plant for hydrogen production. To understand the SI decomposer, a three-dimensional conjugate heat transfer, chemical and fluid flow numerical model was developed in this paper.

The main purpose of the article is to develop a numerical model that can perform design optimization of a SI heat exchanger and decomposer. A preliminary parametric study of the heat exchanger and decomposed design is conducted to explore effects of varying design parameters on the rate of chemical decomposition and stresses.

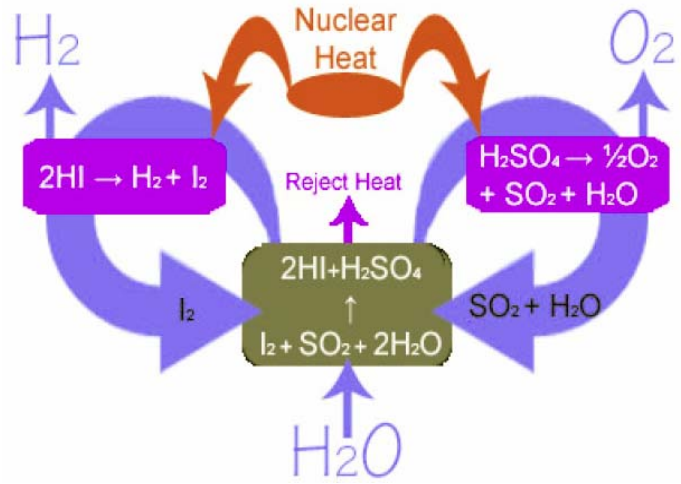

Figure 1. Sulfur-Iodine Thermo Chemical Water Splitting Cycle [8]

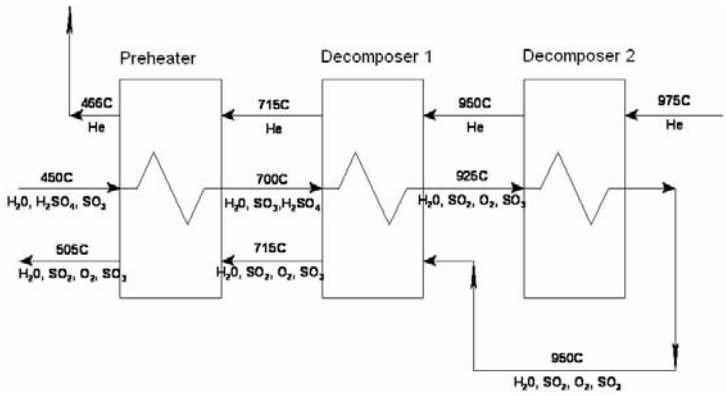

Figure 2. Process Design [5]

SHELL AND PLATE HEAT EXCHANGER AND DECOMPOSER

The design of the shell, plate heat exchanger and decomposer was developed by Ceramatec Inc. (Salt Lake City, USA) and is shown in the Figure 3, [12]. The hot helium from nuclear reactor (T=975°C) is used to heat the SI feed components (H_2O, H_2SO_4, SO_3) to get appropriate condition for the SI decomposition reaction (T>850°C).

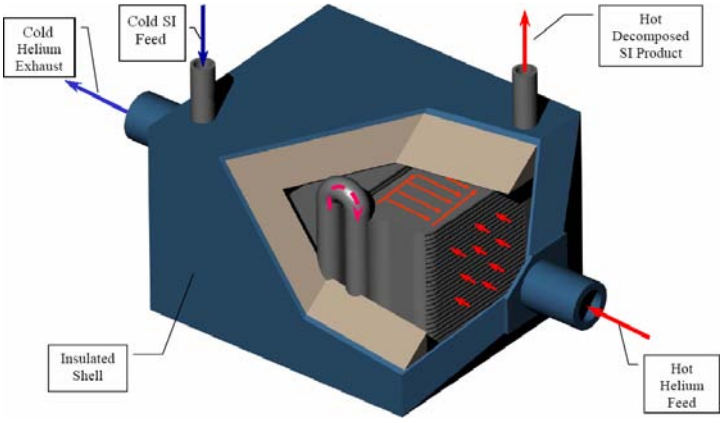

Figure 3. Shell and plate heat exchanger and decomposer [12]

This paper addresses the analysis of Decomposer 1 (Figure 2). Decomposer 1 is chosen because of its complex nature when comparing to Preheater and Decomposer 2 due to the presence of chemical reactions. The assembly of Decomposer 1 is shown in the Figure 4. The layers of Decomposer 1 are shown in the Figure 5.

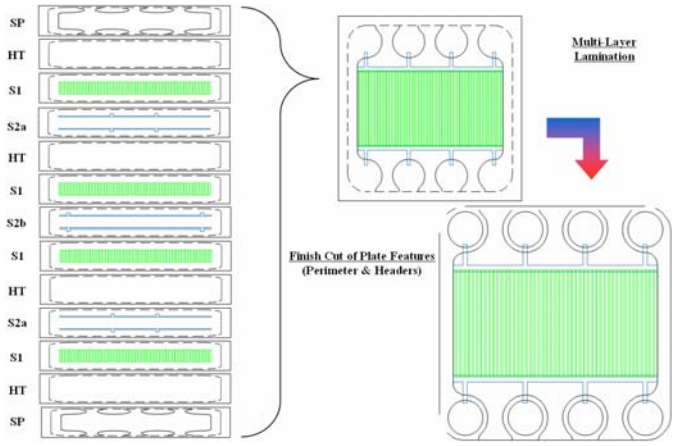

Figure 4. Schematic of Decomposer 1 assembly [12]

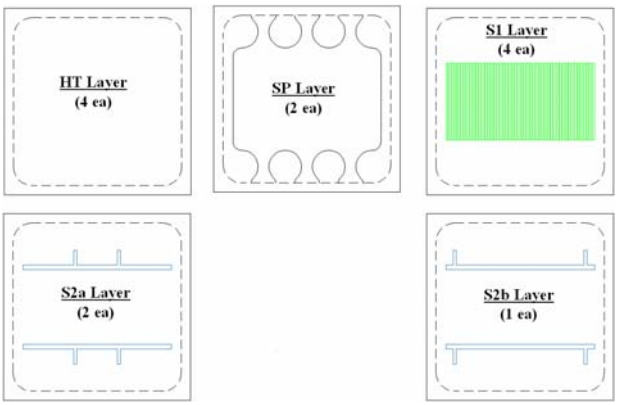

Figure 5. Layers of Decomposer 1 [12]

Development of single channel model

Preliminary CFD analysis showed that mass flow rate in all channels can be almost uniform with proper design of channel manifolds. Therefore, because of the complexity of the overall model, a single channel model is developed. This model includes only half of an internal channel, Figure 6. Such geometry is suitable for the parametric investigation. The original dimensions for the geometry (basis case) are:

$h_{SP} = 0.85\,mm$; $h_{HT} = 0.3\,mm$; $h_{S1} = 0.424\,mm$;

$h_{HT+S2a} = 0.75\,mm$; $h_{1/2\,S2b} = 0.225\,mm$;

$W_1 = 0.635\,mm$; $W_2 = 0.381\,mm$; $L = 52.324\,mm$.

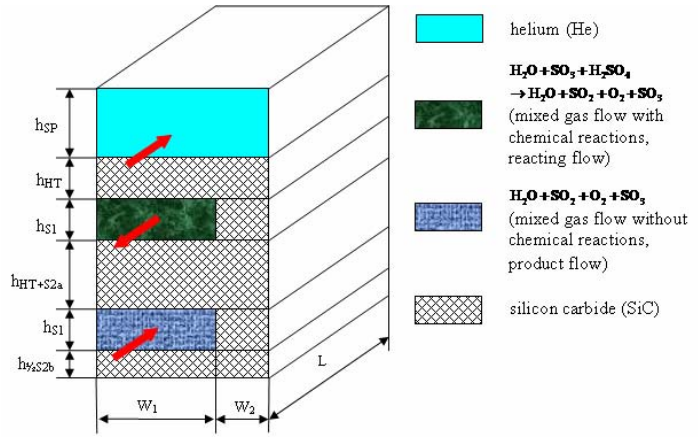

Figure 6. Sketch of the single channel geometry

Geometry and mesh files are created using mesh generator Gambit version 2.0.4. An example of the mesh for the base case is shown in the Figure 7. The mesh has refinements near to interfaces between liquid and solid volumes. Studies are performed to investigate dependence of calculated parameters (pressure, temperature, velocities) on mesh coarseness. Several mesh densities are chosen for this investigation. The current mesh (Figure 7) is found to be suitable.

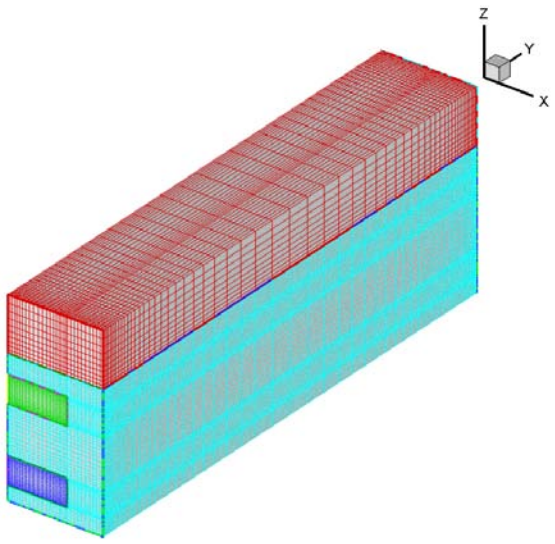

Figure 7. Mesh and computational area (163735 nodes 145800 cells)

Boundary and operation conditions

The boundaries of the calculation domain are shown in the Figure 8.

Inlet conditions for He part:

$\dot{m}$ =2.8175·10^{-6} kg/sec; T=1223.15°K (950°C).

SI inlet for reacting flow:

$\dot{m}$ =6.296·10^{-6} kg/sec; T=974.9°K (701.75°C); $x_{SO_3} = 0.8163$;

$x_{SO_2} = 0$; $x_{O_2} = 0$; $x_{SO_3} = 0.1837$

SI inlet for non-reacting flow:

$\dot{m}$ =6.296·10^{-6} kg/sec; T=974.9°K (701.75°C); $x_{SO_3} = 0$;

$x_{SO_2} = 0.6532$; $x_{O_2} = 0.1631$; $x_{SO_3} = 0.1837$

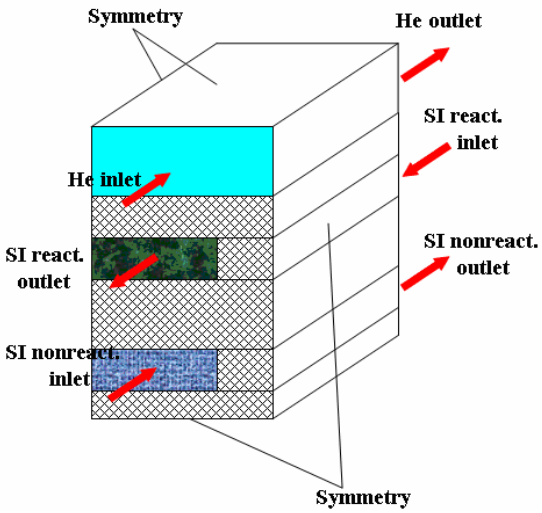

Figure 8. Schematic of boundaries

The boundary conditions on the top, bottom, left and right sides are planes of symmetry. The thermal boundary conditions for the front and back sides are adiabatic conditions. Inlet velocity profiles are uniform and they were calculated by using area, density and mass flow rate. For outflow conditions, the pressure-outlet boundary conditions are used (pressure outlet boundary conditions require the specification of a static (gauge) pressure at the outlet boundary; all other flow quantities are extrapolated from the interior). The operation pressure is 1.5 MPa.

Material properties

According to [6], the thermal conductivity of the SiC depends from temperature significantly. Polynomial interpolation for the thermal conductivity of the SiC is used according to the following:

$$k_{SiC} = 1.94777\cdot10^{2} - 3.60612\cdot10^{-1}\cdot T + 3.30843\cdot10^{-4}\cdot T^{2} - 1.46006\cdot10^{-7}\cdot T^{3} + 2.47588\cdot10^{-11}\cdot T^{4} \quad (4)$$

The density and specific heat of the SiC do not depend on the temperature significantly. Therefore, the properties are assumed as constant for the design temperature range properties for the temperature range (973~1223ºK):

ρ_{SiC}=3130 kg/m^3; Cp_{SiC}=1200 J/(kg·K).

The mixed gas properties for flow areas with and without chemical reactions (see Figure 6) are calculated using Fluent 6.2.16 [9]. The mass fractions for the each component are calculated using:

$$X_i = \frac{\phi_i M_i}{\sum_{i=1}^{n} \phi_i M_i} \quad (5)$$

For density calculation of the mix, the "ideal gas" option is used. For the calculation of molecular viscosity, specific heat, and thermal conductivity of the mix, the "mixing gas" law is used.

Method of solution

All calculations are performed using FLUENT software version 6.2.16 [9]. The solution of the velocity field is accomplished using the SIMPLE algorithm that results in a faster convergence of the iterations. Conjugate heat transfer (which includes conduction through the material and convection through the fluids) is used in order to solve the energy equation. No other thermal boundary conditions are required for the problem since the solver calculates heat transfer directly from the solution in the adjacent cells. In the present study, a general curvilinear coordinate grid generation system is used to discretize the computational domain into a finite number of control volumes (Figure 7). The governing equations for continuity, momentum and energy in the computation domain can be expressed as follows:

$$\frac{\partial}{\partial w_i}(\rho u_i) = 0 \quad (6)$$

$$\frac{\partial}{\partial w_i}(\rho u_i u_k) = \frac{\partial}{\partial w_i}\left(\mu \frac{\partial u_k}{\partial w_i}\right) - \frac{\partial p}{\partial w_k} \quad (7)$$

$$\frac{\partial}{\partial w_i}(\rho u_i T) = \frac{\partial}{\partial w_i}\left(\frac{\lambda}{Cp}\frac{\partial T}{\partial w_i}\right) \quad (8)$$

With proper control of the grid density, the computational domain can be considered for four main regions. The first order upwind numerical scheme is used to discretize the governing equations. For the calculations of the base case geometry the chemical reaction model is used.

Chemical reaction modeling

The governing equation for different species involved in the reaction modeling can be written as follows:

$$\frac{\partial}{\partial w_j}\left(\rho D_{i,m}\frac{\partial X_i}{\partial w_j} - \rho u_j X_i\right) + P_i + S_i = 0 \quad (9)$$

Sulfuric acid dissociates nearly completely into water and sulfur trioxide above 350°C (see [7]), therefore for these calculations the only sulphur trioxide decomposition reaction model ($2SO_3 \rightarrow 2SO_2 + O_2$) was applied. The platinum catalyst is used to enhance decomposition. The wall surface reaction model is implemented to determine the mole fraction of SO_3, SO_2, H_2O and O_2. The reaction rate was defined by follows, [5]:

$$K = A_r\, e^{\left(\frac{-Er}{RT}\right)} \quad (10)$$

For the platinum catalyst $E_r = 8.8034\cdot10^7$ J/kmol; A_r=0.6218

Stress Analysis

In this model, the temperature distribution of the solid part was imported to ANSYS [10] by using the FLUENT's volume mapping function, [9]. Thermal loads are used to calculate stresses in the solid part of the model. A uniform pressure of 1.5 MPa is applied to all surfaces that are adjacent to fluid flow.

The heat exchanger material tensile strength varies with temperature according the following equation, [6],

$$s_{ut} = (0.0142857)T + 200 \qquad MPa \quad (11)$$

Ultimate compressive strength is,

$$s_{uc} = -3\, s_{ut} \quad (12)$$

Figure 9 shows the boundary conditions used in stress analysis. A uniform mesh, Figure 10, is used to calculate stresses. The mesh is chosen after mesh stability studies are performed.

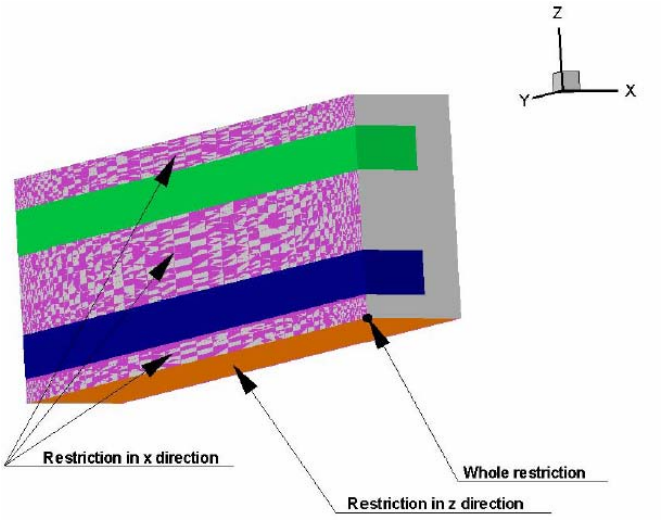

Figure 9. Displacement restrictions for the stress analysis

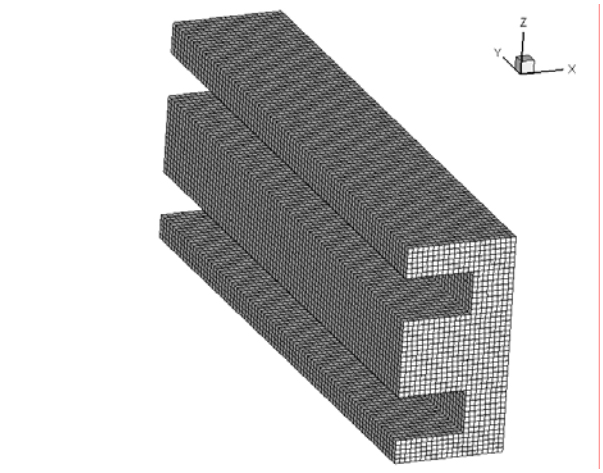

Figure 10. Computation mesh for the stress analysis (63342 nodes 55200 cells)

A MATLAB code is created to calculate the distribution of factor of safety using Coulomb-Mohr failure criteria, [11]. The program imports nodal principal stresses and temperatures as well as element nodal connectivity data and volumes. It follows these steps to calculate the factor of safety:

A. Substitute nodal temperature into equation (11) and Equation (12) to calculate the material strength at each node.
B. Substitute principal stresses into the appropriate Coulomb-Mohr equation at each node.
C. Export factor of safety values for each node back to ANSYS for plotting.
D. Calculate an average factor of safety for each element using the following formula:

$$fse_i = \frac{\sum_{j=1}^{8} fsn_j}{8} \qquad (13)$$

E. Calculate an overall factor of safety performance measure for the heat exchanger in the form of:

$$PM = \frac{\sum_{i=1}^{n_e} fse_i \; v_i}{\sum_{i=1}^{n_e} v_i} \qquad (14)$$

RESULTS OF THE BASIC DESIGN

The flow calculations with sulfur trioxide decomposition ($2SO_3 \rightarrow 2SO_2 + O_2$) for the one channel geometry with platinum catalyst is performed. The calculation domain and boundaries are shown in Figure 11. Figure 12 shows that SO_3 mass concentration is reduced in the reacting flow channel. On the other hand, Figure 13 and Figure 14 indicate that mass concentrations of SO_2 and O_2 respectively increase along the reacting flow direction. Mass concentrations of the reaction products at the outlet of the reaction channel are:

$x_{SO_2} = 0.0033$

$x_{O_2} = 0.00083$

According to the model, the decomposition rate of the sulfur trioxide (SO_3) is extremely small (0.515%). Most likely, the reasons for such small decomposition are:

a) high activation energy for the catalyst;
b) short residence time of the reactant;
c) small area of the chemical reaction with catalyst;
d) relatively low temperature for the chemical reaction (less than 850°C).

Therefore, it is necessary to vary parameters of the current decomposer design to increase decomposition rate of the chemical reaction.

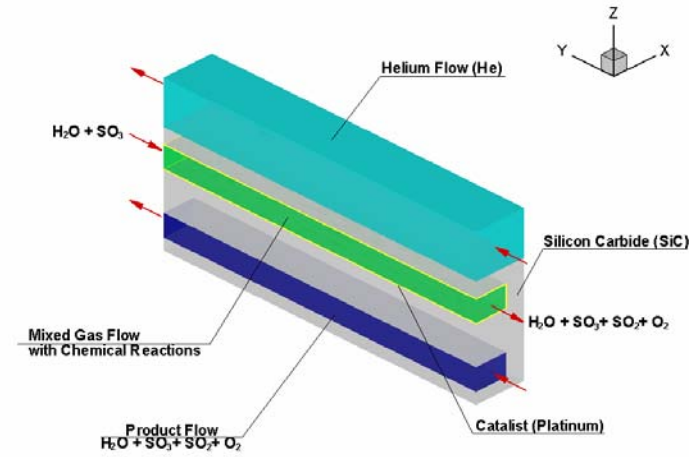

Figure 11. Calculation domain and boundaries

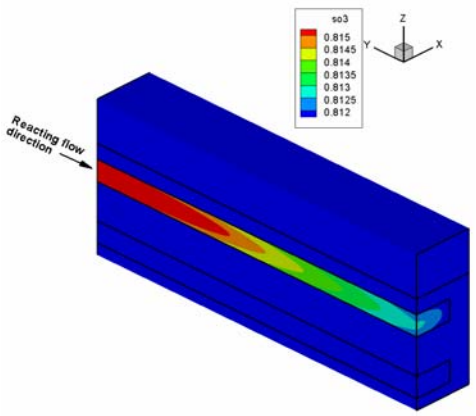

Figure 12. Mass fraction of SO_3

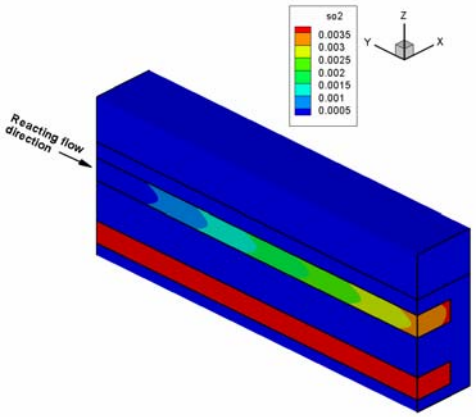

Figure 13. Mass fraction of SO_2

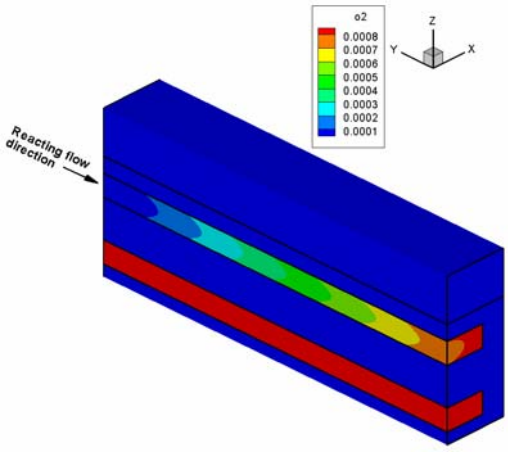

Figure 14. Mass fraction of O_2

Figure 15 through Figure 17 show the nodal solution for the three principal stresses associated with the applied thermal and pressure loads. Figure 18 shows that the resulting nodal factor of safety is extremely high, as the decomposer does not experience significant thermal gradient effects. Calculated overall factor of safety PM (see 14) equals 182.4820.

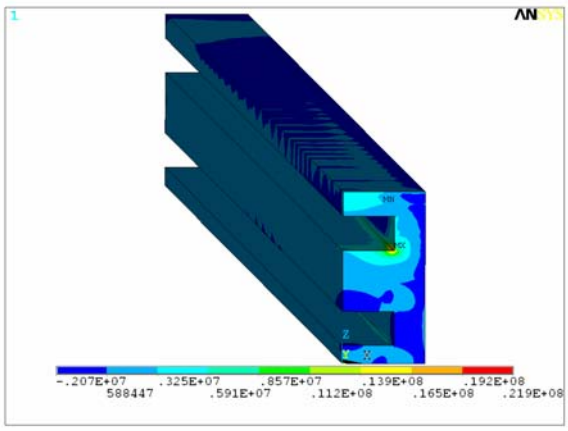

Figure 15. First Principal stress distribution, Pa

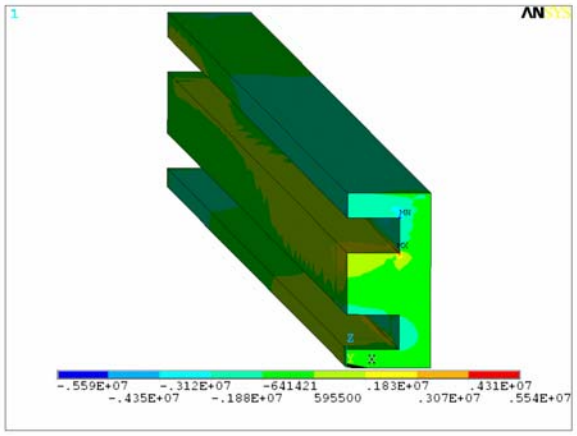

Figure 16. Second Principal stress distribution, Pa

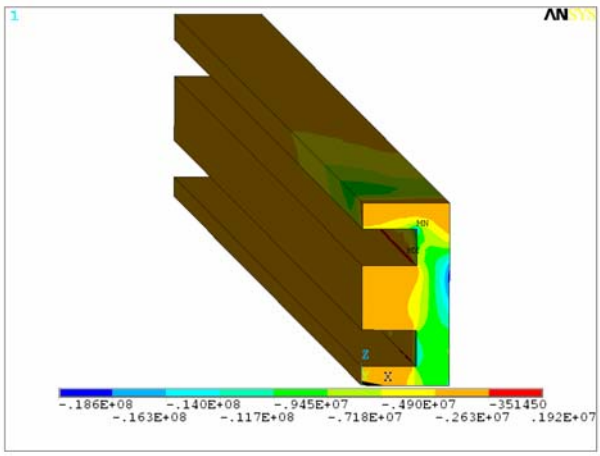

Figure 17. Third Principal stress distribution, Pa

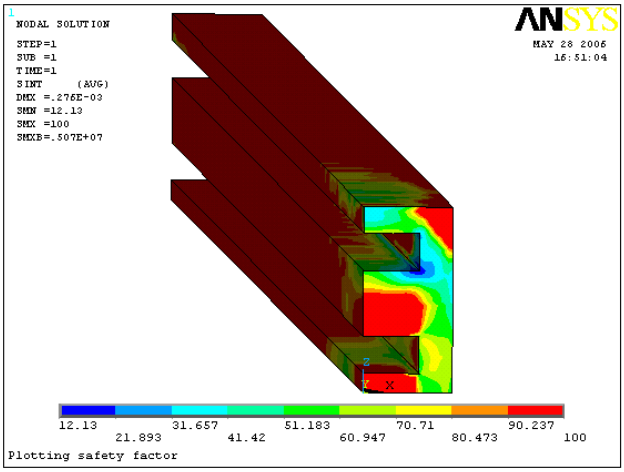

Figure 18. Factor of Safety Based on Coulomb-Mohr failure criteria

PARAMETRIC STUDY OF THE SI DECOMPOSER DESIGN

The calculations for different mass flow rates of mix flow and channel length are performed. Figure 19 shows that percentage decomposition of SO_3 increases significantly as the mass flow rate of the reacting flow decreases. The result is consistent with the general observation that the slower the flow, the residence time of the reactant increases. The percentage decomposition of SO_3 also depends on the channel length as shown in Figure 20. According to this figure, the decomposition rate increases linearly with the increase of the channel length. Resulting stresses are of the same order as those presented in the previous section when either parameter is varied.

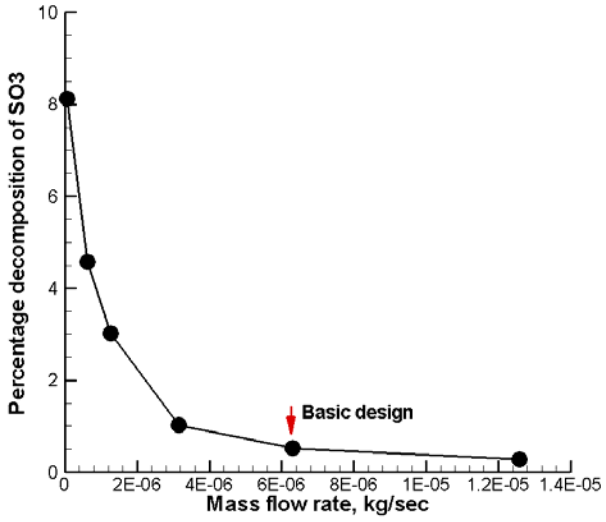

Figure 19. Percentage decomposition of SO_3 versus different mass flow rates in the reacting flow

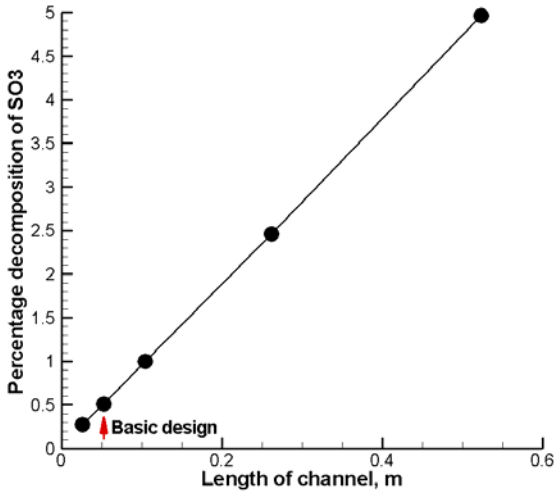

Figure 20. Percentage decomposition of SO_3 versus channel length

CONCLUSIONS

SI decomposer is an important part of the proposed hydrogen production plant. The decomposer performs sulfur trioxide decomposition ($2SO_3 \rightarrow 2SO_2 + O_2$). A three-dimensional computational model for chemical reaction, fluid flow, and heat transfer within a single channel, with platinum catalyst, of the decomposer is developed. Resulting temperature distribution within this model is imported to another finite element analysis software and used along with pressure loads to calculate stresses. For SO_3, a decomposition rate of 0.515% is achieved.

A parametric study is performed on the basic design. Variation of mass flow rates in the reacting flow channel and overall length of the decomposer are considered. Results show that decomposition rates can be increased significantly with reducing reactants mass flow rate and with increasing channel length.

REFERENCES

[1] Brown L., Besenbruch G., Lentsch R., Schultz K., Funk J., Pickard P., Marshall A. and Showalter S, High Efficiency Generation of Hydrogen Fuels using Nuclear Power—Final Technical Report for the Period August 1, 1999 through September 30, 2002, Prepared under the Nuclear Energy Research Initiative (NERI) Program grant no. DE-FG03-99SF21888 for the US Department of Energy, June. 2003.

[2] Hahn D., Design Features of Advanced Sodium-Cooled Fast Reactor KALIMER-600, Proceedings of the 2004 International Congress on Advances in Nuclear Power Plants (ICAPP2004). Pittsburgh, PA, USA, June. 2004

[3] Shimizu S., Nakajima H. and Kubo, K., A Study of the Thermochemical IS process, Organization for Economic Cooperation and Development, The First Information

Exchange Meeting on Nuclear Production of Hydrogen, Paris, France, October. 2000.
[4] Shiozawa S., Ogawa M., Iganaki Y., Present Status of JAERI's R&D on Hydrogen Production Systems in HTGR, Organization for Economic Cooperation and Development, The First Information Exchange Meeting on Nuclear Production of Hydrogen, Paris, France, October 2000
[5] General Atomics Report by Project Staff, Decomposition of Sulfuric Acid Using Solar Thermal Energy, February 1985
[6] Munro R. G., Material properties of a Sintered a-SiC, Journal of physical and chemical reference data, v 26, n 5, p 1195-1203. 1997.
[7] Tagawa H. and Endo T., Catalytic Decomposition of Sulfuric Acid using Metal Oxides as the Oxygen Generating Reaction in Thermochemical Water Splitting Process. International Journal of Hydrogen Energy, v 14, n 1, p 11-17. 1989.
[8] Nuclear Hydrogen Initiative. Ten Year Program Plan. Office of Advanced Nuclear Research. DOE Office of Nuclear Energy, Science and Technology. March 2005
[9] FLUENT Inc, FLUENT 6.2 User's Guide, 2005, Lebanon, NH.
[10] ANSYS, Inc, ANSYS 10. User's Guide, 2004, Canonsburg, PA.
[11] Juvinall, R. and Marshek, K., Fundamentals of Machine Component Design, Wiley, 2006.
[12] Wilson, M., Ceramatec Inc., private correspondence.